794

Construction and Operation of an Axion Helioscope

Letter of Intent

to the

Fermi National Accelerator Laboratory

Lawrence Livermore National Laboratory
University of California at Berkeley
Lawrence Berkeley Laboratory
Texas Accelerator Center
Texas A&M University
Ohio State University
CERN

March, 1988

Construction and Operation of an Axion Helioscope

Letter of Intent
to the
Fermi National Accelerator Laboratory

K. van Bibber (spokesman)
Lawrence Livermore National Laboratory

G. G. Raffelt
University of California at Berkeley

D. M. Moltz
Lawrence Berkeley Laboratory

F. R. Huson and J. T. White
Texas Accelerator Center

P. M. McIntyre
Texas A&M University

R. N. Boyd
Ohio State University

H. N. Nelson
CERN

March, 1988

ABSTRACT

We are preparing and evaluating a design for a detector sensitive to axions and other light particles with a two-photon interaction vertex. Such particles would be produced in the solar interior by Primakoff conversion of blackbody photons and could be detected by their reconversion into x-rays (average energy about 4 keV) in a strong macroscopic magnetic field. The heart of the detector would be the superconducting magnet presently used in the FNAL 15 foot bubble chamber. We envision that the experiment would be sited underground, possibly in the Gran Sasso Laboratory. Assuming the GUT relationship between the axion mass m_a and its two-photon coupling strength, this experiment is sensitive, in principle, to the range $0.1\,\mathrm{eV} < m_a < 5\,\mathrm{eV}$, a regime previously thought to be inaccessible by terrestrial experiments. The range $1\,\mathrm{eV} < m_a$ is excluded by the concordance of calculated and observed lifetimes of helium burning red giants. The observation of the neutrino pulse from the supernova 1987a excludes a range of axion masses between around $10^{-3}\,\mathrm{eV}$ and $1\,\mathrm{eV}$, with considerable uncertainty, however. Thus axions may still exist in the mass range in which our experiment is sensitive. A negative search result would close one of the few remaining windows for axion parameters and thus contribute to an ultimate decision of whether or not the Peccei-Quinn mechanism to solve the CP problem of strong interactions is realized in nature. Considerable work will be required over the next several months to refine background estimates and detection strategies to demonstrate that the necessary signal-to-noise ratio can be achieved over the entire above parameter range. We request assistance from Fermilab to assess the impact of relocation of the bubble chamber magnet and the engineering design required for the proposed use.

TABLE OF CONTENT

1. Introduction

a) Motivation

The conservation of the CP symmetry in strong interactions has been a long standing puzzle of particle physics in view of the CP violating effects observed in the K° meson system. In a compelling theoretical scheme proposed by Peccei and Quinn (1977a,b), the measured absence (or extreme smallness) of the neutron electric dipole moment is linked to the existence of a hitherto undetected particle—the axion (Weinberg 1978, Wilczek 1978). The phenomenological properties of this light, neutral pseudoscalar are mainly determined by the Peccei-Quinn parameter (or axion decay constant) f_a which arises as the scale at which the global chiral $U(1)$ symmetry postulated by Peccei and Quinn is spontaneously broken. Although it was originally thought that f_a should be identified with the electroweak scale $f_{\rm weak} \approx 250\,{\rm GeV}$ ("standard axions"), the axion decay constant can take on, in principle, any value between the GeV range and the Planck scale. Since the interaction strength of axions with matter and radiation scales as $1/f_a$, axion models with $f_a \gg f_{\rm weak}$ are generically referred to as "invisible axions". Depending upon the assumed value for f_a, the existence of axions would lead to a startling variety of phenomenological consequences in particle physics, astrophysics, and cosmology. The compound evidence from these different fields now excludes large ranges of f_a values, leaving open only rather narrow windows in which axions might still exist. Thus it has become a compelling task to attempt the detection of axions in these remaining ranges of parameters, or else to exclude the Peccei-Quinn mechanism once and for all as not being realized in nature.

b) Principle of the detector

We have made a preliminary design of an experiment which relies on the two photon coupling of axions or other light, exotic particles. This vertex allows for the Primakoff conversion (Fig. 1) of photons into axions and vice versa in the presence of external electric or magnetic fields. Thus axions would be produced in the solar interior where blackbody photons (temperature $T = 1.3\,{\rm keV}$ in the solar center) would be converted in the fluctuating electric fields of the charged particles in the hot plasma. These keV axions could be converted into x-rays in the presence of a strong magnetic field in the laboratory ("axion helioscope", Sikivie 1983). We propose to use the FNAL 15 foot bubble chamber magnet for this purpose with a typical magnetic field strength of 3 Tesla and a field volume of about $40\,{\rm m}^3$. Since the magnetic field varies only over macroscopic scales, the axion-photon conversion is best visualized as a mixing

phenomenon (Raffelt and Stodolsky 1988) between these states in the presence of the external field: a state initially known to be an axion would subsequently oscillate, in part, into a photon. One easily finds that the transition rate is largest when the axion and photon are "degenerate", i.e., when their dispersion relations are identical so that the axion and photon component of a beam remain in phase for as long a distance as possible. In a medium, the dispersion relation for photons is identical with that of a massive particle if the photon energy is far above all resonances of the constituents of the medium. For x-rays in the keV range and a low-Z gas such as hydrogen or helium, this condition is met with sufficient precision so that one can match the axion mass with an effective photon mass over the whole range of relevant frequencies. Also, the absorption of x-rays by the medium (the imaginary part of the dispersion relation) is then so small that the x-ray component is not strongly damped over meter distances in our detector. The experiment would be operated in a scanning mode where the pressure of the gas is varied in appropriate steps such as to cover an interval of possible axion masses. In summary, the main ingredients of our detection scheme are

- the sun as an axion source,
- a strong magnetic field to mix the axion with the photon for reconversion,
- hydrogen or helium gas at variable pressure to match the axion and photon dispersion relation in order to enhance the transition rate,
- and a large area array of detectors sensitive to single photons in the $1 - 10\,\mathrm{keV}$ range, with a very low background rate.

c) Relevant parameter range

Our experiment would be sensitive to at least one decade of f_a values in a regime that covers one of the remaining parameter ranges in which axions may still exist. It is convenient to discuss the relevant parameter ranges in terms of the axion mass m_a by virtue of a universal relationship between m_a and f_a,

$$m_a = 1.2\,\mathrm{eV}\ N\,(10^7\,\mathrm{GeV}/f_a)\,, \tag{1}$$

where N is a non-zero, model-dependent integer coefficient of the color anomaly of the axion current*. We closely follow the normalization of parameters of Srednicki

* Note that the axion coupling to gluons, which is at the heart of the Peccei-Quinn scheme, is given as $(\alpha_s/4\pi)(N/f_a)G\tilde{G}a$ with the strong fine structure constant α_s and the axion field a. Thus the generic parameter governing different axion models is f_a/N which is uniquely represented by the axion mass.

(1985). The axion photon interaction is given as

$$\begin{aligned}\mathcal{L}_{a\gamma\gamma} &= -\frac{\alpha}{4\pi}\frac{N}{f_a}\,(E/N-1.92)\,a\,F_{\mu\nu}\tilde{F}^{\mu\nu} \\ &= -\frac{(m_a/\mathrm{eV})\,(E/N-1.92)}{2.1\times10^{10}\,\mathrm{GeV}}\,a\,F_{\mu\nu}\tilde{F}^{\mu\nu}\,,\end{aligned} \tag{2}$$

where E is the coefficient of the electromagnetic anomaly of the axion current. Note that $F_{\mu\nu}\tilde{F}^{\mu\nu} = -4\,\mathbf{E}\cdot\mathbf{B}$ and a is the axion field. In all grand unified axion models $E/N = 8/3$ and we shall refer to this value as the GUT relationship between the axion mass and the photon coupling strength. Other values for E/N are possible, however, and specifically $E/N = 2$ would lead to a large suppression of the photon coupling strength (Kaplan 1985). For GUT axions with $E/N = 8/3$ our range of sensitivity is

$$0.1\,\mathrm{eV} < m_a < 5\,\mathrm{eV}\,. \tag{3}$$

We stress, however, that generally our detection scheme depends on both the axion mass and the axion-photon coupling strength, and that these two parameters are *not* universally related because of the unknown value of E/N. Thus it is frequently convenient to express the axion-photon interaction as

$$\mathcal{L}_{a\gamma\gamma} = -\frac{1}{4M}\,a\,F_{\mu\nu}\tilde{F}^{\mu\nu} = \frac{a\,\mathbf{E}\cdot\mathbf{B}}{M}\,, \tag{4}$$

where M is given by $M^{-1} = |(\alpha/\pi)(N/f_a)(E/N-1.92)|$. Typical values of interest are m_a in the eV range and M in the $10^{10}\,\mathrm{GeV}$ range. With the notation $M_{10} = M/10^{10}\,\mathrm{GeV}$ one finds that

$$\frac{1}{M_{10}} = \frac{E/N-1.92}{8/3-1.92}\times 1.45\,(m_a/\mathrm{eV})\,. \tag{5}$$

For purposes of clarity we shall usually confine our discussion to the case of GUT axions with $E/N = 8/3$ while an ultimate analysis of the experimental results would fully explore the two-dimensional (M, m_a) parameter space. Such a discussion would then also cover more general cases of hypothetical particles besides axions.

d) Competing astrophysical arguments

Our range of sensitivity overlaps, in part, with regimes excluded by astrophysical arguments although we believe that axions can still exist in our parameter range. Raffelt and Dearborn (1987) show in a detailed discussion of stellar evolution that

the existence of axions would lead to a severe conflict between calculated and observed lifetimes of helium burning red giants unless $M > 1\times10^{10}\,\mathrm{GeV}$. It is assumed that axions are lighter than about 10 keV so that their emission from the stellar plasma would not be Boltzmann suppressed. For GUT axions, this excludes the range

$$0.7\,\mathrm{eV} \lesssim m_a \lesssim 10\,\mathrm{keV}\,. \tag{6}$$

It is thought that the uncertainty in this bound—aside from the unknown value of E/N—does not exceed a small factor of order unity. This argument addresses the axion-photon coupling and thus compares most directly with our experiment.

There exist very restrictive constraints on the axion-electron coupling from late neutron star cooling (Iwamoto 1984), from the observed white dwarf cooling time scale (Raffelt 1986), and from the suppression of helium ignition in low mass red giants (Dearborn, Schramm, and Steigman 1986). The translation into axion mass bounds is somewhat model dependent. Typically, the range

$$0.03\,\mathrm{eV} \lesssim m_a \lesssim 10\,\mathrm{keV} \tag{7}$$

would be excluded. However, axions do not need to couple to electrons at tree level ("hadronic axions", Kaplan 1985), and then these results are irrelevant. Thus in our range of interest, only hadronic axions could still be expected to exist. Therefore we shall confine our attention to this type of model with important implications for the calculation of the solar axion spectrum (see Sect. 2 below).

Another argument relevant to our regime arises from late neutron star cooling (Iwamoto 1984, Tsuruta and Nomoto 1986). One finds a bound on the axion-nucleon coupling which translates, somewhat model-dependently, into an excluded regime for the axion mass of about

$$0.01\,\mathrm{eV} \lesssim m_a \lesssim 10\,\mathrm{keV}\,. \tag{8}$$

This result, however, is invalidated if nucleon superfluidity occurs in the interior of neutron stars, as is frequently assumed. Then the emission rate from the relevant nucleon bremsstrahlung processes is strongly suppressed. Other uncertainties associated with this bound arise from the unknown equation of state for dense nuclear matter and from the uncertain determination of the surface temperature of pulsars of known age.

The argument which "competes" most severely with our proposed experiment arises from the observation of a neutrino pulse from the supernova 1987a. This measurement indicates that the gravitational binding energy released in the collapse

of the progenitor star was carried away by neutrinos, thus limiting the interaction strength of axions and other weakly interacting, exotic particles (Raffelt and Seckel 1988, Turner 1988, Mayle *et al.* 1988). However, if axions interact too "strongly" they are "trapped" in the hot proto neutron star that has formed after collapse just like neutrinos so that they would be inefficient in carrying away the energy stored in the supernova core. The excluded regime translates, in a model-dependent fashion, into a regime of excluded axion masses,

$$0.001\,\mathrm{eV} \lesssim m_a \lesssim 3\,\mathrm{eV}\,. \tag{9}$$

The upper end of this window where axions would be "strongly" interacting and trapped in the SN core has been estimated by Turner (1988). The uncertainty in this range is rather severe, perhaps as much as an order of magnitude on either end of the window. This means that the actually excluded regime may be much smaller than stated in Eq. (9). Also, however, the regime where axions would be important for SN dynamics could be much larger than the range Eq. (9).

The main uncertainties are: (a) The small number and uncertain energies of the observed neutrinos, the unknown value of the electron neutrino mass, and the uncertain distance to the Large Magellanic Cloud all of which prohibit the precise determination of the time and energy structure as well as the absolute normalization of the neutrino *emission* spectrum at the SN. (b) Uncertainties in the calculation of the axion-nucleon interaction processes in dense nuclear matter. (c) Uncertainties in theoretical SN modelling. (d) The model-dependent translation between the axion-nucleon interaction strength and the axion mass. (e) The lack of a self-consistent treatment of SN models including axions. Note that the (self-consistent) treatment of Mayle *et al.* (1988) only addresses the lower end of the range Eq. (9) in a specific axion model, while only Turner (1988) gives an *estimate* of the upper end which is most relevant for the "competition" with our experiment.

While some of these uncertainties can be removed by a more detailed study of SN models including the effect of axions, it appears that there may well exist a window for the existence of axions between the red giant bound and the SN bound. It is remarkable that our experiment addresses precisely this range where a new and reliable axion search would considerably extend our knowledge about the question of the axion's existence.

e) Other axion experiments

Other experiments that address the question of the axion's existence mainly operate

in the regime of f_a values near $f_{\rm weak}$—for a review see Cheng (1987) and Davier (1987). The experimental exclusion of axions in this regime has lead to the notion that axions must be "invisible" if they exist. For very large values of f_a (very small axion masses), an axion condensate would have formed in the early universe, and unless $f_a/N \lesssim 10^{12}$ GeV, i.e., $m_a \gtrsim 10^{-5}$ eV, the universe would be "overclosed" by axions (Preskill, Wise, and Wilzcek 1983, Abbott and Sikivie 1983, Dine and Fischler 1983). Near saturation of this bound, axions would constitute the "cold dark matter" that is believed to dominate the universe. Then axions clustered in our galaxy could be detected by their magnetic conversion into microwaves in a high-Q cavity (Sikivie 1983). An experiment of this sort is under way and has produced first negative results (DePanfilis *et al.* 1987), at a level, however, not relevant for the relationship between the axion mass and the photon coupling strength Eq. (2). Although this galactic axion search is of paramount importance for particle physics and cosmology, it is not clear at present whether it will be possible to "touch the axion line" Eq. (2) in the near future. For m_a of a few eV, thermally produced axions in the early universe would have survived in large numbers. Their present-day decay would be visible as a "glow" of the night sky (Kephart and Weiler 1987, Turner 1987), and existing measurements of the brightness of the night sky exclude a window of axion masses in the eV range. Another recently proposed experiment (Maiani, Petronzio, and Zavattini 1986, Melissinos *et al.* 1987) which addresses the magnetically induced birefringence of the vacuum will not be able to probe a regime covered by Eq. (2). Aside from measurements of the brightness of the night sky, our experiment is thus the only laboratory method sensitive to realistic axion models in the "far invisible" regime.

f) Summary

We believe, in summary, that the construction and operation of an axion helioscope would substantially extend our knowledge about the existence or non-existence of axions and the realization of the Peccei-Quinn mechanism in nature. The uncertainties of the astrophysical bounds, in conjunction with the freedom of the relevant parameters of the axion models, appear to be sufficiently severe to warrant an independent experimental effort. It is remarkable that our search would be most sensitive in a regime where two very different astrophysical arguments may or may not overlap. A detection of axions in this range—aside from its paramount importance for particle physics—would then be of great importance for astrophysics while a negative search result would allow one close the potential gap between these arguments with confidence. We thus proceed to discuss details of the experiment.

2. The Sun as an axion source

a) The axion spectrum

If we confine our attention to hadronic axion models where these particles do not interact with electrons at tree level, they can be efficiently produced in the Sun only by processes involving their two photon coupling Eq. (4). In the interior of the Sun, blackbody photons can convert into axions in the fluctuating electric fields of the charged particles in the plasma (Raffelt 1988)—see Fig. 1. In the limit of a large momentum transfer, this process can be viewed as the Primakoff effect on isolated charges. For a small momentum transfer, it is better visualized as the interaction with coherent field fluctuations in the plasma (longitudinal plasmons). The total transition rate of a photon (or rather transverse plasmon) of energy ω into axions is found to be

$$\Gamma(\gamma\to a) = \frac{T\,\kappa^2}{(4\pi M)^2}\,\frac{\pi}{2}\left[\left(1+\frac{\kappa^2}{4\omega^2}\right)\ln\left(1+\frac{4\omega^2}{\kappa^2}\right)-1\right], \tag{10}$$

where T is the temperature of the plasma. The Debye-Hückel scale κ is given by

$$\kappa^2 = (4\pi\alpha/T)\sum_j Z_j^2 N_j\,, \tag{11}$$

where N_j is the number density of charged particles with charge $Z_j e$. The inverse of κ is the screening scale for charges in a plasma while κ defines the borderline between a "large" and a "small" momentum transfer in the axion production process. The energy of the axion is close to the energy of the original photon because of the non-relativistic motion of the charged particles: the energy is smeared over an interval with a width on the order of the plasma frequency $\omega_{\rm pl}^2 = (4\pi\alpha/m_e)\,N_e$ with the number density N_e of electrons. A detailed result for the energy smearing is given in Raffelt (1988). Numerically, in the solar center one has $T = 1.3\,\mathrm{keV}$, $\omega_{\rm pl} = 0.3\,\mathrm{keV}$, and $\kappa = 9\,\mathrm{keV}$.

The axion luminosity of the Sun is now determined by folding the photon-axion transition rate Eq. (10) with a blackbody photon distribution. To this end we have ignored the small spread of the axion energies for a given photon energy. Then we have integrated over a standard solar model (Bahcall *et al.* 1982) and find the differential axion flux as plotted in Fig. 2 (solid line). The average axion energy is $\langle E_a\rangle = 4.2\,\mathrm{keV}$. With the notation $M_{10} = M/10^{10}\,\mathrm{GeV}$ the total flux at the Earth is found to be

$$F_a = 3.54\times10^{11}\,\mathrm{cm}^{-2}\,\mathrm{sec}^{-1}/M_{10}^2\,. \tag{12}$$

The total energy flux (luminosity) in axions is

$$L_a = 1.7\times10^{-3}\, L_\odot / M_{10}^2\,, \tag{13}$$

where $L_\odot = 3.86\times10^{33}\,\mathrm{erg\,sec^{-1}}$ is the solar (photon) luminosity. Thus axion production would cause only a very minor perturbation of the sun. The differential axion spectrum at the earth is well approximated by

$$\frac{dF_a}{dE_a} = \frac{1}{M_{10}^2}\, 4.02\times10^{10}\,\mathrm{cm^{-2}\,sec^{-1}\,keV^{-1}}\, \frac{(E_a/\mathrm{keV})^3}{\mathrm{e}^{E_a/1.08\mathrm{keV}}-1} \tag{14}$$

where E_a is the axion energy—see the dashed line in Fig. 2. Note that this is *not* a thermal spectrum which would vary as $E_a^2/(e^{E_a/T}-1)$. Note also that the difference between the result of our numerical integration and our analytical approximation to this result is negligible in view of the approximations involved in our calculation.

b) The angular divergence of the axion flux at the earth

In our proposed experimental setup the conversion between axions and x-rays would take place in long, relatively thin tubes so that an aperture effect occurs. Thus we need to determine the angular divergence of the axion radiation at the earth which arises because of the spatial extension of the axion source. To this end we have calculated the radial distribution of the axion production rate over the standard solar model of Bahcall *et al.* (1982). In Fig. 3 we show the radial distribution of the axion energy loss rate, dL_a/dr, normalized to unity if integrated from the solar center to the surface. Most axions emerge from a region within $0.2\,R_\odot$ (solar radii) of the solar disk. The average distance beteen the Sun and the earth is $214.9\,R_\odot$, corresponding to one astronomical unit or $1.50\times10^{13}\,\mathrm{cm}$. Thus the angular radius of the axion source region as viewed from the earth is $\delta_a \approx (0.2/214.9)\,\mathrm{rad} = 0.9\times10^{-3}\,\mathrm{rad}$.

3. Axion-photon conversion rate

a) Equation of motion

We now proceed to calculate the axion-photon conversion rate in the presence of a nearly homogeneous magnetic field and a refractive medium. To this end we consider the propagation of a wave ψ, the dispersion relation of which is close to that of a massless particle. Moreover, we consider a definite frequency component ω and plane

wave propagation in z direction only. Then one may use a linearized form of the wave equation (Raffelt and Stodolsky 1988), $i\partial_z\psi = n\omega\psi$, where n is the refractive index for this wave. For relativistic particles with mass m it is given as $n = 1 - m^2/2\omega^2$ so that the momentum of the particle is $|\mathbf{k}| = \omega - m^2/2\omega$. We are concerned with a situation where ψ is a two-component vector and n is a 2×2 matrix with generally complex entries.

If one considers the propagation of axions and photons in the presence of a (nearly homogeneous) magnetic field $\mathbf{B}$, one finds from very general arguments (Raffelt and Stodolsky 1988) that only the photon component with polarization parallel to the magnetic field mixes with axions*. Denoting the amplitude of this parallel photon component with A and the amplitude of the axion field with a, our linearized wave equation reads (Raffelt and Stodolsky 1988)

$$i\partial_z \begin{pmatrix} A \\ a \end{pmatrix} = \begin{pmatrix} n_\gamma\omega & B_t/2M \\ B_t/2M & \omega - m_a^2/2\omega \end{pmatrix} \begin{pmatrix} A \\ a \end{pmatrix} \tag{15}$$

with B_t the component of $\mathbf{B}$ transverse to the wave vector $\mathbf{k}$, and M is defined by Eq. (4). The photon refractive index n_γ is, in general, complex because of absorptive effects in the medium.

b) An upper limit to the expected x-ray flux

Assuming, at first, that the diagonal entries of this matrix were real and equal, assuming a homogeneous field, and that the beam contains only an axion component at the beginning of the field region, one easily finds that after a distance ℓ the probability of measuring a photon is given as

$$p(a\to\gamma) = |B_t\ell/2M|^2 . \tag{16}$$

This approximate result holds only if $p \ll 1$. For $B_t = 3$ Tesla and $M = 1\times10^{10}$ GeV we find $B_t/2M = 1.48\times10^{-12}\,\mathrm{cm}^{-1}$ so that for path-lengths in the meter range this condition is well-satisfied. This transition rate sets an absolute ceiling to what one can achieve with a given field strength and a given path length. All effects which occur from the non-equality of the diagonal entries in our mixing matrix reduce this

* By "parallel" component we mean the polarization state whose electric field vector lies in the plane of the wavevector $\mathbf{k}$ and the magnetic field $\mathbf{B}$. It is parallel to $\mathbf{B}$ only if the propagation is strictly transverse to the magnetic field.

result. Taking now $B_3 = B_t/3\,\text{Tesla}$, $\ell_4 = \ell/4\,\text{m}$, and again $M_{10} = M/10^{10}\,\text{GeV}$, an absolute ceiling to the expected x-ray flux from solar axion conversion is thus

$$F_\gamma = 1.2\times10^{-7}\,\text{cm}^{-2}\,\text{sec}^{-1}\,B_3^2\ell_4^2/M_{10}^4 \tag{17}$$

where we have used the result Eq. (12). This result sets the scale for the x-ray fluxes we are concerned with. The x-ray spectrum would follow Eq. (14) with an appropriate normalization.

c) General result for the transition rate

In general, the dispersion relations for axions and photons are not identical. However, for x-rays in the keV range and for a low-Z gas as a medium, photons propagate approximately like massive particles. Thus we write for the photon refractive index

$$n_\gamma\omega = \omega - m_\gamma^2/2\omega - \mathrm{i}\Gamma/2\,, \tag{18}$$

where m_γ may vary in space because of density gradients of the medium, and it also contains a weak residual dependence on ω. Γ is the damping coefficient, or inverse absorption length, for the x-rays so that the intensity of a beam decreases as $\mathrm{e}^{-\Gamma z}$. The quantities m_γ and Γ are easily related to the usual atomic scattering factors f_1 and f_2 as tabulated, e.g., by Henke *et al.* (1982). In order to determine a general solution to the "Schrödinger equation" Eq. (15) we make use of the "perturbed wavefunction" approach outlined by Raffelt and Stodolsky (1988). Note, however, that the "Hamiltonian" in Eq. (15) is not Hermitian so that one has to modify the procedure to solve this equation accordingly. From a first order perturbative solution we then find for the transition *amplitude*, aside from an overall phase,

$$\begin{aligned}\langle A(z)|a(0)\rangle = (1/2M)\,\exp\Big\{-\int_0^z dz'\Gamma/2\Big\}\times \\ \times\int_0^z dz' B_t\,\exp\Big\{\mathrm{i}\int_0^{z'} dz''\Big[(m_\gamma^2 - m_a^2)/2\omega - \mathrm{i}\Gamma/2)\Big]\Big\}\,.\end{aligned} \tag{19}$$

This result is first order in the small quantity $B_t z/2M$, but completely general otherwise. Note that, in general, B_t, Γ, and m_γ are functions of z. If we now assume that all of these quantities are constant in space, and if we introduce the oscillation length by

$$2\pi/\ell_{\text{osc}} = |(m_\gamma^2 - m_a^2)/2\omega| \tag{20}$$

the transition rate is found to be, for a path length $z = \ell$,

$$p(a \to \gamma) = \frac{(B_t/2M)^2}{(2\pi/\ell_{\rm osc})^2 + \Gamma^2/4} \left[1 + e^{-\Gamma\ell} - 2e^{-\Gamma\ell/2}\cos(2\pi\ell/\ell_{\rm osc})\right]. \qquad (21)$$

In the absence of damping ($\Gamma = 0$) this is the usual result for the transition between two mixed particle states.

4. The detector

4.1 Basic concept

The heart of the detector would be the FNAL 15 foot bubble chamber magnet: coil and cryostat, refrigerator and helium inventory. Possibly we will also want the vacuum tank and the bubble chamber itself.

Since the Primakoff effect is an $\mathbf{E} \cdot \mathbf{B}$ interaction, it is important that the magnetic field be perpendicular to the line-of-sight to the sun to maximize the conversion probability. This implies that we will want to mount the axis of the Helmholtz pair at an angle $90° - \Theta_{\rm latitude}$, on the average at least, and if possible allow for the equinoctial variation of $\pm 23°$.

Inside of the magnet bore is a vessel containing hydrogen or helium gas for matching of the axion and photon dispersion relations. The rear semicylindrical surface is instrumented with high-efficiency, low-noise detectors for x-rays in the $(1 - 10)$ keV range. The area transverse to the Sun's line-of-sight for which the magnetic field is a meaningful fraction of the central value of 3 Tesla is about $15\,\mathrm{m}^2$. In order that the helioscope have pointing ability there will be a collimator structure, which could be an array of hexagonal close-packed tubes, with the x-ray detectors at the end of each tube. The array of tubes, while costing a small packing fraction factor, are the most attractive option. This is so because the tubes, rather than the tank itself, will serve the role of containing the gas whose pressure will be very great while searching in the higher mass region. Since the *density* determines the index of refraction rather than the *pressure*, we may obtain higher gas densities at lower pressures by cooling the gas. This will necessitate a double-walled cryostat. The tubes should have a diameter of perhaps 3" or so, in order that the aperture effect be negligible. The inner vessel at least will be free-standing from the magnet, as it will have to be gimballed and

continuously rotated to point at the Sun 24 hours a day. A cutaway isometric view of a possible design is shown in Fig. 4.

4.2 Counting rates

To calculate estimated counting rates for the experiment, we have made a simplified model for the detector. We assume that the clear bore of the magnet is 4 m in diameter, that its usable length is 3 m, and that the magnetic field is 3 T everywhere within this volume. We further assume for now that the entire rear semicylindrical surface is instrumented with x-ray detectors of unit efficiency, and we do not worry about lost area due to detector packing fraction, *etc.*, which would introduce a reduction factor of about 0.5.

The pressure required to match the effective mass for x-rays in the medium with the axion mass is found by expressing the real part of the photon dispersion relation by an effective mass in the spirit of Eq. (18),

$$m_\gamma^2 = 4\pi r_0 \, (N_A/A\, m_u)\, \rho f_1 \, . \tag{22}$$

Here r_0 is the classical electron radius, N_A is Avogadro's number, A is the relevant atomic mass number, m_u the atomic mass unit, ρ is the gas density, and f_1 is the real part of the atomic scattering factor as tabulated, e.g., by Henke (1982). The use of the lowest-Z gas possible is clearly indicated on two counts. First, the real part of the atomic scattering factor f_1 is linear in Z, whereas the absorptive part (proportional to the mass attenuation coefficient) increases roughly as Z^3. Second, the variation of $f_1(\omega)$ in the relevant range $\omega = (1 - 10)\,\mathrm{keV}$ is sufficiently weak only for H_2 and He so that the matching of the dispersion relations can be achieved *simultaneously* over this entire range of frequencies. For these gases, the asymptotic value $f_1(\omega \to \infty) = Z$ is taken on with sufficient precision over our entire range of interest. Fig. 5 shows the pressure of either H_2 or He gas as a function of axion mass; note the m_a^2 dependence, as well as the absolute values required for the high-mass end of the scale if the gas is at room temperature. The advertised upper mass limit of our experiment is somewhat arbitrary and determined by the practical issues posed by gas handling at high pressures. The virtue of cooling the gas to liquid Ne temperatures is obvious—compare the right- and left-hand scales of Fig. 5.

For a given mass of the axion, the total conversion rate over the whole rear semicylindrical surface of the detector and over the whole axion spectrum is given by

$$R = H \int dy \int dE_a \, F_a' \, p_{a\to\gamma}[z(y)] \,. \tag{23}$$

Here H is the height and D the diameter of the cylinder instrumented with detectors, F_a' is the differential solar axion flux as given by Eq. (14), and $z(y) = 2\sqrt{(D/2)^2 - y^2}$ is the length of the chord through the cylinder at transverse position y. The conversion rate $p_{a\to\gamma}[z(y)]$ depends on the axion-photon coupling strength, and implicitly on both m_a and E_a through $\ell_{\rm osc}$ as given by Eq. (20). We have incorporated the effect of photon attenuation by using $p_{a\to\gamma}$ as given by Eq. (21). The result is shown in Fig. 6 for the relationship Eq. (2) between m_a and the axion-photon coupling with the assumed GUT value $E/N = 8/3$. Aside from absorptive effects—most evident at large values of m_a and rendering H_2 preferable to He—the overall rate goes as m_a^4. It is seen that for m_a in the eV range, the rate will be large, perhaps many per second. The nominal lower end of our experimental sensitivity in mass, $m_a \approx 0.1\,\text{eV}$, corresponds to a rate on the order of $1\,\text{day}^{-1}$. While again somewhat arbitrary, this lower limit anticipates solutions to the challenge of background reduction to that level.

At a fixed pressure P_0, the response of the detector will be a sharply peaked function of m_a. In Fig. 7 we show the integrated rate as a function of m_a, where the pressure has been optimized for $m_0 = 1.000\,\text{eV}$. The full-width fifth-maximum here is seen to be $(\Delta m/m_0)_{1/5} \approx 0.0022$. Here, Δm is the difference between the actual axion mass m_a and the value m_0 at which the counting rate would be optimal, $\Delta m = |m_0 - m_a|$. It is easy to show that the width of the response curve scales as m_0^{-2} (see Fig. 8). As a rough rule of thumb the full-width half-maximum is approximately $(\Delta m/m_0)_{1/2} \approx 0.0012\,(m_0/\text{eV})^{-2}$. This implies that the experiment will be a *tuning* search in pressure. Later we will comment briefly on the implications for the strategy of the search, the demands on the stability and uniformity of the gas density, and the running time of the experiment.

If axions were found to exist, the spectrum of x-rays measured in the detectors at the rear of the pressurized tube array would faithfully reproduce the axion spectrum (Fig. 2) aside from absorptive effects and assuming the pressure is optimized for the relevant axion mass. If the pressure were set substantially off the maximum of the response curve, the measured spectra and distribution in transverse position y would be modulated non-trivially as the oscillation length $\ell_{\rm osc}(m_a, E_a, P_0)$ became comparable to $z(y)$.

4.3 Detection of x-rays

One of the principle efforts of this experiment will be the R&D of x-ray detectors for the $(1 - 10)$ keV range which can be made cheaply over a large area, have unit efficiency, and extremely low background. We are just at the outset of this study. Unfortunately, the energy of the x-rays is just high enough that clever schemes to reflect and focus x-rays from the entire back semicylindrical surface onto a small Si(Li) detector using multilayer optics will not work (Barbee 1988). Thus it will be necessary to instrument the entire back surface of perhaps $15\,\mathrm{m}^2$.

a) Large area silicon detectors

The most desirable alternative would be the use of large area Si(Li) detectors. The depletion depth would be chosen to provide reasonable efficiency for detecting few-keV x-rays, but minimize the Compton scattering of high energy γ-rays from background radioactivity. As the photoelectric cross section is strongly energy-dependent ($\propto E^{-7/2}$), the signal-to-noise ratio may be optimized by a judicious choice of depletion depth. A preliminary analysis roughly favors $10\,\mu$.

If we opt for a hexagonal close-packed tube array, the Si(Li) detectors would be mounted inside and would only require a feedthrough at the back wall of the tube. As the tubes will be on the order of 3" diameter, this implies around 2500 such silicon detectors. The unit price for such a large detector normally is very high (around $ 1000.00) in small orders. However, we have had informal discussions with a company in Southern California concerning our application, and it seems possible that in large quantity the price may fall by an order of magnitude. Of course, the contractual product specifications and factory diagnostics would be much more relaxed than those for small orders of devices for high-resolution spectroscopy. We are optimistic concerning this possibility.

b) Inorganic scintillators

The next most attractive concept would be the use of very thin crystals of an inorganic scintillator, e.g., CsI(Tl) in conjunction with one or more large area ($1\,\mathrm{cm}^2$) PIN diodes. CsI for photon detection has been undergoing a renaissance in recent years, e.g., the CLEO II electromagnetic calorimeter will be fabricated of CsI(Tl). It has the highest photon yield of any known material, 52 photons/keV (Holl 1987), it is only mildly hygroscopic, unlike NaI(Tl), and it is easy to work with. Two features of CsI give room for optimism that the background rate may be kept low. First, a disk of CsI could be fabricated of the minimum thickness necessary to stop essentially

all of the x-rays, i.e., about 15 mg/cm^2, which will also stop all of the resulting photoelectrons even at the highest energy of importance to us. This will minimize the Compton scattering, *etc.* from natural radioactivity. Second, the long decay time of the scintillation (about 900 ns at 300° K, and longer at very low temperatures) gives us pulse shape information. By digitizing the same signal both for a "long" and a "short" ADC gate, one should be able to discriminate against the prompt signals that would be due to either Cerenkov light in the optical coupling medium between the scintillator and the diode, or direct conversion in the diode itself. Large area PIN diodes (the Hamamatsu S 1790-02) can be cooled to reduce the dark current well below the signal level, and the unit cost will certainly be manageable (about $ 30.00). The unfortunate aspect of this scheme is that the photon statistics in a non-ideal geometry would probably preclude any useful energy resolution: this would be an x-ray *counter* rather than a *spectrometer.*

c) Proportional chambers

The third avenue that will be explored, but about which we are least sanguine, is the use of Ar or Xe proportional chambers at the end of the pressurized tube array. Since x-rays will be readily absorbed by all but the thinnest films, it is clear that the pressure of the Ar or Xe proportional chamber will have to track the ballast gas (H_2 or He) precisely and reliably over three orders of magnitude in pressure range. Otherwise the window will be blown out or in. Furthermore, proportional mode operation will have to be demonstrated over the entire dynamic range displayed in Fig. 5, the last decade of which, we believe, is without precedent. Finally, the integrity of the window will have to be absolute: even the most minute amount of Ar or Xe leaking into the ballast gas for a particular tube would radically decalibrate the relationship between pressure and index of refraction, which ultimately is what must be controlled and monitored to within some fractional bandwidth in mass.

4.4 Engineering considerations

This section comprises a list of some of the more challenging technical aspects of the experiment concerning materials, design and construction, operation, monitoring, and others. Although we have not decided upon specific courses, we mention them to indicate that we are aware of the issues, have begun to address them seriously, and are optimistic about their solution.

a) Pressurized tubing array

In Fig. 5 we showed the operating pressure of either H_2 or He gas as a function of axion mass for two different temperatures, one at Standard Temperature (273° K), and the other at LNe (27° K). It is clear that at room temperature, the pressure for searching in the several eV range will be formidable, $P_0 \approx 4000\,\text{psi}$ at $m_a = 4\,\text{eV}$. Chrome-nickel stainless steel piping for plant processing applications in the several-inch diameter range have a typical wall thickness-to-diameter ratio of about 0.14 for 4000 psi. As this scales roughly with pressure, one may estimate that the weight of the tube array alone would be roughly $8(m_{\text{max}}/\text{eV})^2$ tons, where m_{max} is the upper limit of the mass search. Thus for 5 eV as the upper limit of the experiment, the tube array would weigh about 200 tons! Additionally, stainless steel is notorious for the amount of radioactive contaminants it contains. This would probably be unacceptable in the present application.

An attractive option would be to cool the pressurized tube array to liquid nitrogen temperatures, and perhaps one could even contemplate liquid neon. This would have very significant beneficial effects. It would permit the use of much thinner walled material, because the pressure would be reduced by a factor of 4 (at 77° K), and because all materials increase considerably in allowable stress when cooled. Then a number of alternative "clean" materials (titanium or even synthetic composites) could be used.

b) Gimballing

The requirement of pointing the helioscope at the Sun necessitates that the vessel containing the tube array and detectors be free-supported from the magnet, and rotate smoothly at 15° per hour. The materials and drive mechanism must be designed keeping in mind the strong unclamped magnetic field of the 15' bubble chamber magnet (0.25 kG at 5 m).

Since the conversion probability scales with B_t^2, it is very important to be able to orient the axis of the coil at an angle with respect to vertical, and preferably that this angle be adjustable. The support of the coils in the cryostat was not designed to take up large shear forces—a problem that needs to be studied.

c) Vacuum tank and cold vessel for the detector

The detector will probably be designed for cryogenic operation, requiring a double-walled vessel. In Fig. 4 we show a possible scheme, with both walls within the clear bore of the magnet. Other options include the use of the existing vacuum tank and the bubble chamber itself in our design.

d) Temperature uniformity and monitoring

For the coherent conversion of axions into photons it is important that the gas density be equal along the length of each tube. Since the gas will be static, and all the tubes will communicate with one another through their respective feed lines from a manifold, the entire experiment is guaranteed to be isobaric. The pressure gradient due to gravity—the "law of atmospheres"—is negligible in the present case so that isodensity is equivalent to isothermality.

To a lesser degree it is desirable that the density of all tubes be the same. If this is not satisfied, the situation can be recovered so long as the thermistry permits accurate knowledge of the density (and thus index of refraction) of each tube. Assuming the existence of the axion in our range of sensitivity, as one scans different tubes would go through the conversion resonance at values of the pressure slightly displaced from one another. However, a significant density gradient along one single tube itself implies an averaging or smearing of its response curve. In practice, as the orientation of the tubes is at an arbitrary angle, it is difficult to imagine having each tube as an isotherm without having the entire array (of a few meters linear dimension) as an isotherm.

The mass bandwidth translates into a condition on the temperature uniformity according to $\Delta T/T = 2\Delta m/m_0$. Again, m_0 is the axion mass for which the detector response at a chosen pressure P_0 is optimal. If one does not wish to smear the response of any tube beyond the full-width half-maximum of the resonance, this implies $\Delta T/T < 0.002\,(m_0/\mathrm{eV})^{-2}$. For the smallest masses, where the expected counting rate is very low, the bandwidth in mass is largest. In fact, the bandwidth in mass is quite large at the lower mass limit of this experiment, about 0.1 at $m_0 = 1\,\mathrm{eV}$. One might argue that the temperature uniformity condition is needlessly stringent at the higher mass (few eV) end: one could afford smearing over a much wider fraction of the mass as the absolute conversion rate would be expected to be acceptably large even far down on the tails of the resonance. Such an argument should be viewed with caution: the relation between m_a and the axion-photon coupling is not known *a priori* and indeed there are models where the axion-photon coupling may be highly suppressed ($E/N = 2$, Kaplan 1985). Strictly adhering to the condition that the response curve not be averaged beyond its FWHM implies a temperature uniformity of $6°$ mK at LN_2, for $m_0 = 5\,\mathrm{eV}$. This small value for the maximum allowable deviation from temperature uniformity and the requisite monitoring is potentially a problematic point with cryogenic operation.

We will examine how good an isotherm one can hope to achieve for the proposed geometry. The first obvious candidate would be a cryogenic bath with a gas-liquid

interface above the tops of the tubes. The other is a cooled minimum two-point support for the array inside a cryo/vacuum vessel. In addition to the radiative and possible conductive inward heat flow, we have to assess the importance of the heat source represented by the reverse current of thousands of silicon diodes.

4.5 Backgrounds

The ultimate limit to the sensitivity of the proposed search is set, on the low-mass end, by background. Background events can be generated by three sources, radioactivity in the materials of the detector and its environment, cosmic ray interactions, and detector noise. Radioactivity is by far the most serious background in a deep underground environment. The main background rate of the detector is then a product of three factors,

- The total rate R_γ of the photons traversing the detector elements due to radioactivity,
- the probability P_c that these photons scatter within a detector element, and
- the probability P_x that the signal produced is indistinguishable from a few-keV x-ray.

Measurments in the Gran Sasso laboratory indicate a photon background from the rock of $r_0 \approx 30\,\mathrm{Hz/kg}$. Of comparable importance may be the background from the magnet coil itself, which has not yet been measured, because it will also nearly surround the detector. Taking for now only the contribution from the surrounding rock, a rough approximation yields $R_\gamma \approx r_0\,\lambda\,A/2 \approx 15\,\mathrm{kHz}$. Here, λ is the mean free path of a 500 keV γ-ray, $\lambda \approx 10\,\mathrm{g/cm^2}$, and $A/2 \approx 5\,\mathrm{m^2}$ is the average solid angle-area product subtended by the detector elements. By a carefule choice of shielding and building materials (pre-war steel, virgin lead, etc.) we hope to reduce this locally to $R'_\gamma \approx 500\,\mathrm{Hz}$.

Regarding the probability for scattering in the detector elements, a Compton cross section of about 5 barns and a depletion depth of $10\,\mu$ in a Si(Li) detector yield the *total* Compton probability of $P_c \approx 2.5\times10^{-4}$.

In order to estimate what fraction P_x of the scattered γ-rays ($E_\gamma \approx 500\,\mathrm{keV}$) will be indistinguishable from a low-energy x-ray ($E_x \approx 5\,\mathrm{keV}$), we assume that the Compton spectrum is flat. Thus $P_x \approx E_x/E_\gamma \approx 10^{-2}$.

However, we envision a geometry by which each detector element will be backed by about $2\,\lambda$ of active shielding, e.g., NaI with a photodiode, giving us an additional Compton suppression of $P_{\rm shield} \approx 0.15$.

Taking all of these factors together, we find a total background counting rate of

$$R_{\rm background} = R'_\gamma\, P_c\, P_x\, P_{\rm shield} \approx 2{\times}10^{-4}\,{\rm Hz}\,. \tag{24}$$

This corresponds to a rate of roughly $16\,{\rm day}^{-1}$. We note that at $m_a = 0.1\,{\rm eV}$ the expected signal would be on the order of $1\,{\rm day}^{-1}$. Given the roughness of our present estimates, it is clear that a much more careful study of the background rates is needed to establish the possibility of reaching, indeed, our advertised lower end of 0.1 eV.

4.6 Operational strategy

This experiment is a *tuning* experiment by which the ballast gas pressure P_0 is varied in order to enhance the conversion probability of the axion into an x-ray, over a narrow window in mass. A detailed *strategy* of how to allocate search time is premature as it depends critically on knowledge of backgrounds. Nevertheless, we can estimate the total number of discrete steps which the experiment will require, and the total time, assuming we wish to see 1 "true" event per mass "window".

If the pressure P_0 is set such that the conversion rate is optimal for a mass m_0, this rate is approximately

$$R(m_0) = 3{\times}10^{-2}\,{\rm sec}^{-1}\,(m_0/{\rm eV})^4\,. \tag{25}$$

The fractional full width half maximum of the response curve as a function of the actual axion mass m_a is

$$F_{1/2}(m_0) = (\Delta m/m_0)_{1/2} \approx 10^{-3}\,(m_0/{\rm eV})^{-2}\,. \tag{26}$$

Thus using only the FWHM of the response curve and ignoring its tails, the relevant number $N_{\rm steps}$ of discrete steps in gas pressure for a range (m_1, m_2) of axion masses is

$$N_{\rm steps} = \int_{m_1}^{m_2} \frac{dm_0}{m_0\, F_{1/2}(m_0)} \approx 500\,(m_2^2 - m_1^2)/{\rm eV}^2 \approx 500\,(m_2/{\rm eV})^2\,. \tag{27}$$

Similarly, the total measuring time $t_{\rm search}$ is given by

$$t_{\rm search} = \int_{m_1}^{m_2} \frac{dm_0}{m_0\, F_{1/2}(m_0)\, R(m_0)} \approx 1.6{\times}10^4\,(m_1^{-2} - m_2^{-2}) \approx 1.6{\times}10^4 (m_1/{\rm eV})^{-2}\,. \tag{28}$$

Thus the total search time would be $t_{\rm search} \approx 20$ days if one attempts to reach to an axion mass of 0.1 eV. This, of course, ignores "off-times" when the magnetic field is off, or the helioscope is pointed away from the Sun, etc., interleaved with the "on-times" so as to continuously monitor backgrounds.

If a candidate axion signal were detected, the detector would be operated at the appropriate mass setting for an extended period of time to improve the signal-to-background ratio, perform a time correlation analysis, and so on. Should the axion then be found to exist, its mass would be determined with extreme accuracy.

5. Proposed initial work and milestones

It is clear that considerable engineering and R&D needs to be performed before the experiment can actually be mounted. Nevertheless we believe that the scientific case for this experiment is firm, both in terms of its niche in the overall axion picture, and in terms of its methodological soundness. Thus we have decided to submit at this PAC to avoid loss of a whole year. We propose to proceed by the following initial plan of work and milestones for the next six months.

5.1 Initial work on the part of FNAL

We request that no permanent disposition of the 15' bubble chamber (magnet, refrigerator, vessels, gaseous inventories, *etc.*) be made until we are able to present a more detailed plan no later than fall of this year. Moreover, we request that a FNAL engineer and designer be committed to develop a plan with us for the disassembly, moving, and setting up of the magnet and ancillary equipment.

5.2 Initial work on our part

We commit ourselves to meet the following goals by the fall of this year.

a) Detector concept and prototype

Decision on the concept as early as possible, and demonstration of a successful prototype x-ray detector for these conditions and geometry.

b) Backgrounds

Over the next several months we will perform a characterization all relevant gamma activities from the existing bubble chamber magnet, proposed construction materials (by sample procurement), and the site environment when determined. The impact of these activities on the actual detectors must be better understood and the lower mass limit of the experiment more clearly determined.

c) Preliminary design

Reasonably final solutions to the issues discussed in Sect. 4.4 can be expected, along with a preliminary design. Particular emphasis must be given to the question of temperature (and thus density) uniformity, and how the detector and tube array will be cooled.

d) Hazards

A preliminary plan will be drafted for addressing the potential hazards associated with various gaseous inventories in areas of confined occupancy.

e) Siting

Possible sites for the experiment both in the U.S. and in Europe will be studied. Backgrounds will be the driving consideration.

f) Collaborators

The collaboration must expand in view of the work to be done. While we expect that more people will be added at the institutions already represented (students and postdoctoral researchers), there is need for another strong group. Fermilab personnel have played a vigorous role in axion searches for the past several years: Rochester-Brookhaven-FNAL microwave cavity dark matter search, BNL E-840 (approved), E-605, E-613 reanalysis, SLAC E-141, and extant FNAL proposal in search of the

GSI 1.8 MeV state in e^+e^-. We would be delighted to have Fermilab collaborators with us and play a strong role in this experiment.

g) Resources

A proposal is in preparation for submission to DOE for funding of the R&D required to evaluate this experiment. Initially this would cover the detector development, engineering studies, and on-site background measurements.

6. Personnel

A preliminary breakdown of the work described in Sect. 6 by institution is described.

a) Lawrence Livermore National Laboratory

LLNL will take responsibility for the engineering of the detector vessel, particularly its cryogenic and solar tracking aspects.

b) University of California at Berkeley

Georg Raffelt has made numerous contributions to the understanding of the astrophysical axion limits, including work on white dwarf cooling, detailed stellar evolution calculations, and bounds from the supernova 1987a. More important for our experiment is his definitive work on the role of plasma effects in stars, which significantly weakened the original bounds on hadronic axions, and which allows for a reliable calculation of the solar axion spectrum from the axion-photon interaction. Also, with L. Stodolsky he has developed the elegant axion-photon mixing formalism and has generalized it to include the effects of photon absorption.

c) Lawrence Berkeley Laboratory

Dennis Moltz has made his career measuring extremely rare and very low-energy nuclear decay modes in hostile environments. He brings considerable experience in background processes, and will be responsible for materials evaluation using LBL's facility for ultra-low γ-counting. While at ORNL, he played precisely this role in an axion experiment which was one of the final blows to the "standard" axion of Weinberg (1978) and Wilczek (1978).

d) Texas Accelerator Center

Russ Huson played a major role in the construction of the 15' bubble chamber magnet and will work with the designated FNAL personnel in scoping the moving and reconfiguration of the magnet.

e) Texas A&M University

The work towards a prototype x-ray detector will be managed by Peter McIntyre. Of the present collaboration he alone has experience in deep-underground physics, having performed a large-volume scintillator monopole search in a salt mine.

f) Ohio State University

Richard Boyd is nearing completion of a novel and competitive neutrino mass experiment, and also performs low-counting rate measurements of astrophysically interesting reactions induced by beams of unstable nuclei. He will be invaluable in understanding and reducing the influence of radioactive backgrounds on our large area detector array.

g) CERN

Harry Nelson (with Karl van Bibber) has published a recent calculation on the limits of invisible axions that could be set in a purely terrestial experiment using the Primakoff coupling. He will be responsible for environmental background measurements at the candidate European sites.

REFERENCES

Abbott, L., and Sikivie, P. 1983, *Phys. Lett.*, **120 B**, 133.

Bahcall, J., *et al.* 1982, *Rev. Mod. Phys.*, **54**, 767.

Barbee, T. W., Jr. 1988, private communication.

Bellotti, E. 1988, *Nucl. Instr. Meth.* **A 264**, 1.

Cheng, H.-Y., 1987, Report IUHET-125, submitted to *Phys. Rep.*

Davier, M. 1987, Report LAL 87-27, to be published.

DePanfilis, S., *et al.* 1987, *Phys. Rev. Lett.*, **59**, 839.

Dearborn, D. S. P., Schramm, D. N., and Steigman, G. 1986, *Phys. Rev. Lett.*, **56**, 26.

Dine M., and Fischler, W. 1983, *Phys. Lett.*, **120 B**, 137.

Iwamoto, N. 1984, *Phys. Rev. Lett.*, **53**, 1198.

Henke, B. L., *et al.* 1982, *Atomic Data and Nuclear Data Tables* **27**, 1.

Holl, I., Lorenz, E., Mageras G. 1987, Report MPI-PAE/Exp. E1.185, presented at the IEEE Nuclear Science Symposium, San Francisco, Oct. 21-23, 1987, and to be published in the IEEE Transactions on Nuclear Science.

Kaplan, D. B. 1985, *Nucl. Phys.*, **B 260**, 215.

Kephart, T., and Weiler, T. 1987, *Phys. Rev. Lett.*, **58**, 171.

Kim, J. E. 1987, *Phys. Rep.*, **150**, 1.

Maiani, L., Petronzio, R., and Zavattini, E. 1986, *Phys. Lett.*, **175 B**, 359.

Mayle, R., *et al.* 1988, submitted to *Phys. Lett. B.*

Melissinos, A. C., etal 1987, Experimental Proposal (approved Brookhaven Experiment E-840).

Peccei, R. D., and Quinn, H. 1977a, *Phys. Rev. Lett.*, **38**, 1440.

Peccei, R. D., and Quinn, H. 1977b, *Phys. Rev. D*, **16**, 1791.

Preskill, J., Wise, M., and Wilczek, F. 1983, *Phys. Lett.*, **120 B**, 127.

Raffelt, G. 1986, *Phys. Lett.*, **166 B**, 402.

Raffelt, G. 1988, *Phys. Rev. D*, to be published.

Raffelt, G., and Dearborn, D. 1987, *Phys. Rev. D*, **36**, 2211.

Raffelt, G., and Seckel, D. 1988, submitted to *Phys. Rev. Lett.*

Raffelt, G., and Stodolsky, L. 1988, *Phys. Rev. D*, in press.

Sikivie, P. 1983, *Phys. Rev. Lett.*, **51**, 1415 (E) *ibid.* **52**, 695 (1984).

Srednicki, M. 1985, *Nucl. Phys.*, **B 260**, 689.

Tsuruta, S., and Nomoto, K. 1986, IAU-Symposium No. 24, *Observational Cosmology*, in press.

Turner, M. 1987, *Phys. Rev. Lett.*, **59**, 2489.

Turner, M. 1988, submitted to *Phys. Rev. Lett.*

Weinberg, S. 1978, *Phys. Rev. Lett.*, **40**, 223.

Wilczek, F. 1978, *Phys. Rev. Lett.*, **40**, 279.

FIGURE CAPTIONS

Figure 1

Feynman diagram for the Primakoff production of axions by the interaction of a photon with an electron or nucleus (top), and (bottom) axion-photon conversion in the electric or magnetic field of an external source denoted by a cross ($\times$).

Figure 2

Differential solar axion flux at the earth. We assume that axions are only produced by the Primakoff conversion of blackbody photons in the solar interior ("hadronic axions"), and we assume a standard solar model (Bahcall *et al.* 1982). The axion-photon coupling strength M is defined in Eq. (4). The solid line arises from a numerical integration over the Sun, the dashed line is an analytical approximation to this result as given in Eq. (14).

Figure 3

Radial distribution of the axion energy loss rate L_a of the Sun, normalized to unity if integrated over the entire sun. The radial coordinate r is in units of the solar radius $R_\odot$.

Figure 4

A cutaway isometric view of the detector.

Figure 5

Pressure of H_2 or He gas to optimize the detection of axions of a given mass. Left-hand vertical axis for $T = 273°$ K, right-hand for $T = 27°$ K (liquid Ne).

Figure 6

Total rate of axion-photon conversion as a function of the axion mass m_a, using Eq. (5) for the relationship between m_a and the axion-photon coupling M and assuming the GUT value $E/N = 8/3$. The pressure is assumed to be optimized for each value of m_a. At the largest m_a values, corresponding to large gas densities, the rate for He (dashed line) is less than that for H_2 (solid line) because of the increased importance of absorption for a higher-Z medium.

Figure 7

Integrated rate as a function of m_a if the gas pressure P_0 has been set to optimize the counting rate for axions of mass $m_0 = 1\,\mathrm{eV}$. The dashed line is a blow-up of the solid line and corresponds to the scale on the upper horizontal axis.

Figure 8

The full-width fifth-maximum "bandwidth" in mass, $(\Delta m_a/m_0)_{1/5}$, as a function of the mass m_0 for which the pressure is optimized.

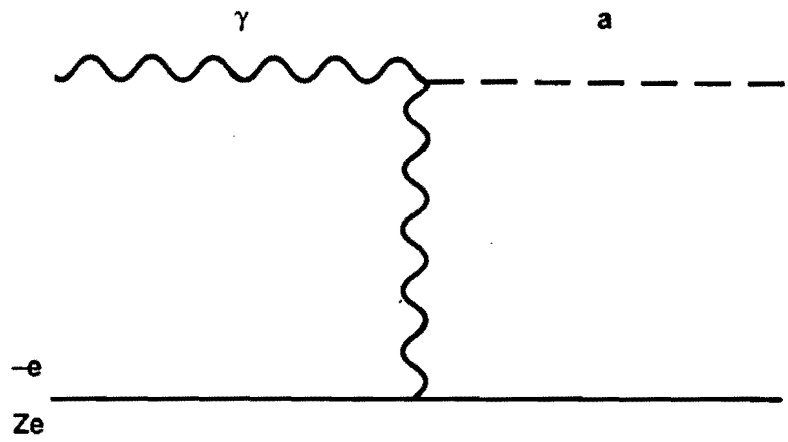

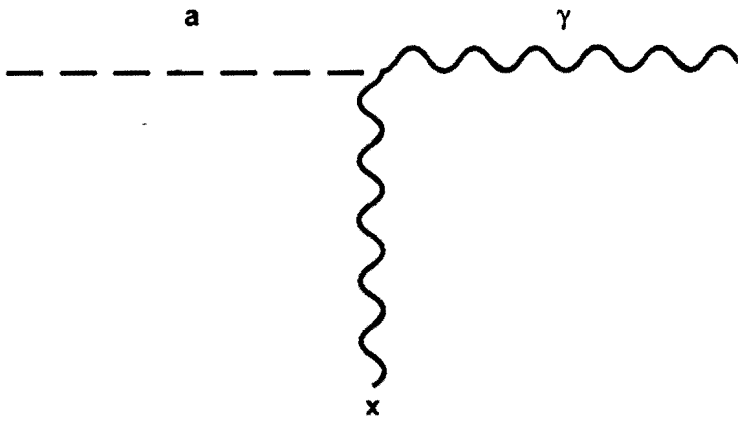

Figure 1

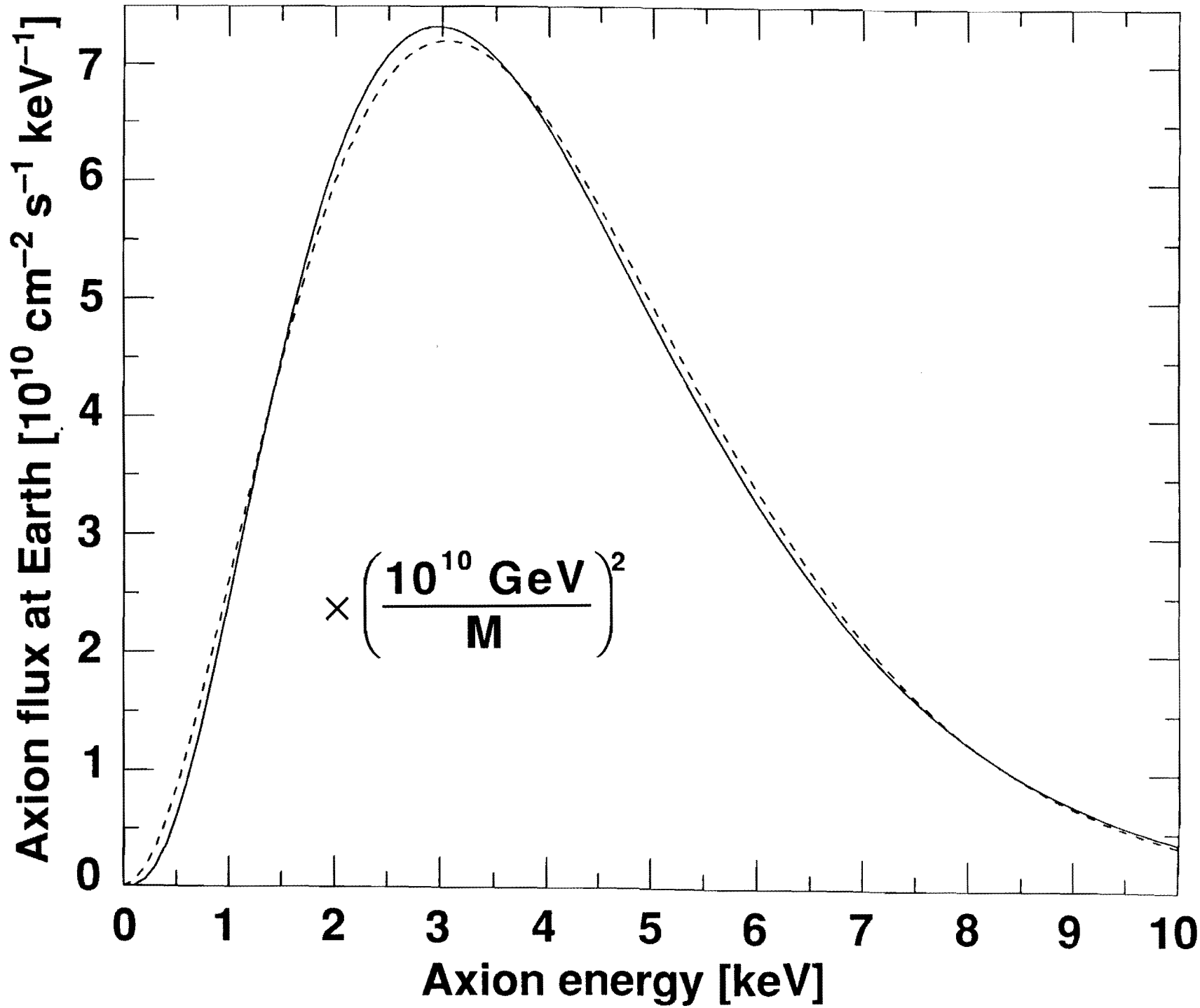
Axion flux at Earth [10^{10} cm^{-2} s^{-1} keV^{-1}]
0
1
2
3
4
5
6
7
$\times \left(\frac{10^{10}\ \text{GeV}}{M} \right)^2$
0
1
2
3
4
5
6
7
8
9
10
Axion energy [keV]

Figure 2

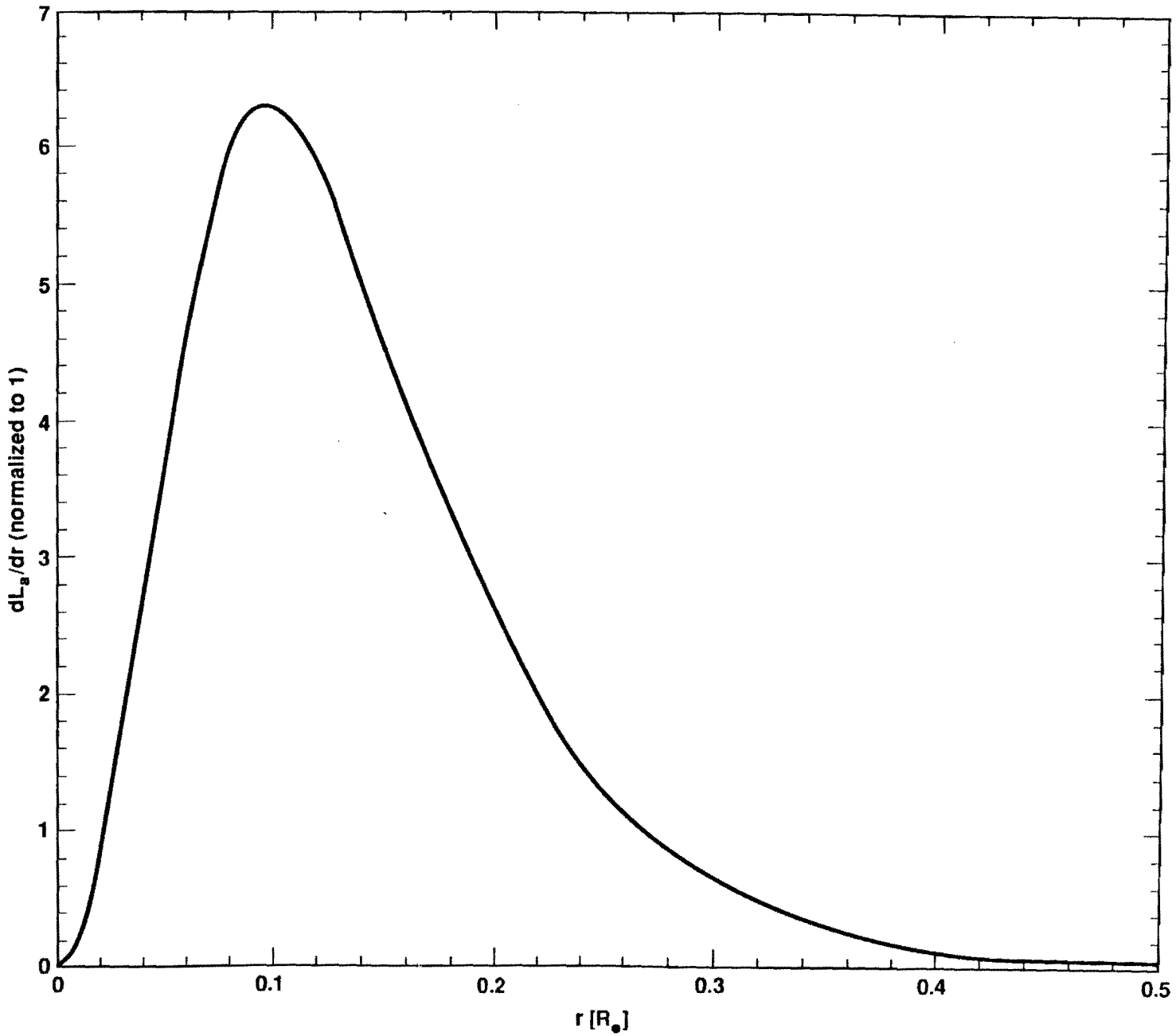

Figure 3

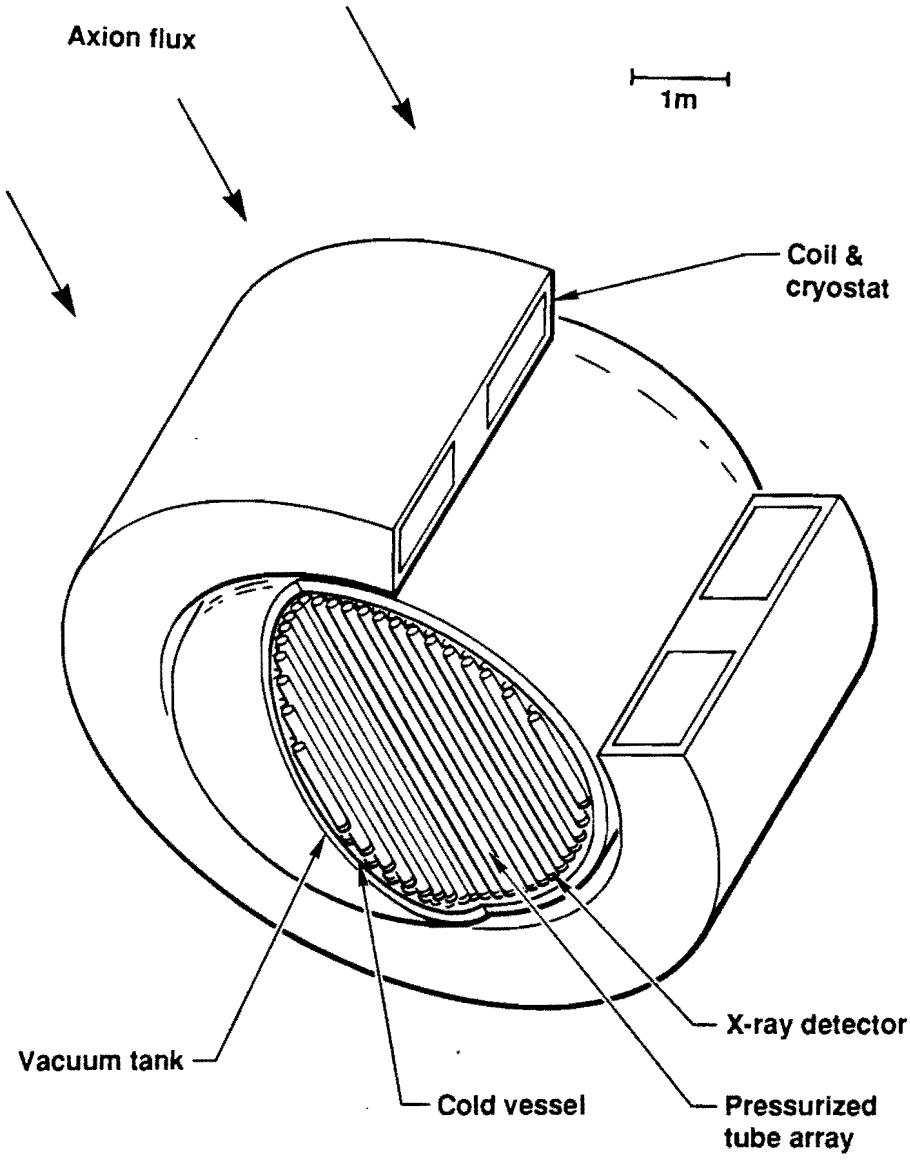
Axion flux
1m
Coil &
cryostat
Vacuum tank
Cold vessel
X-ray detector
Pressurized
tube array

Figure 4

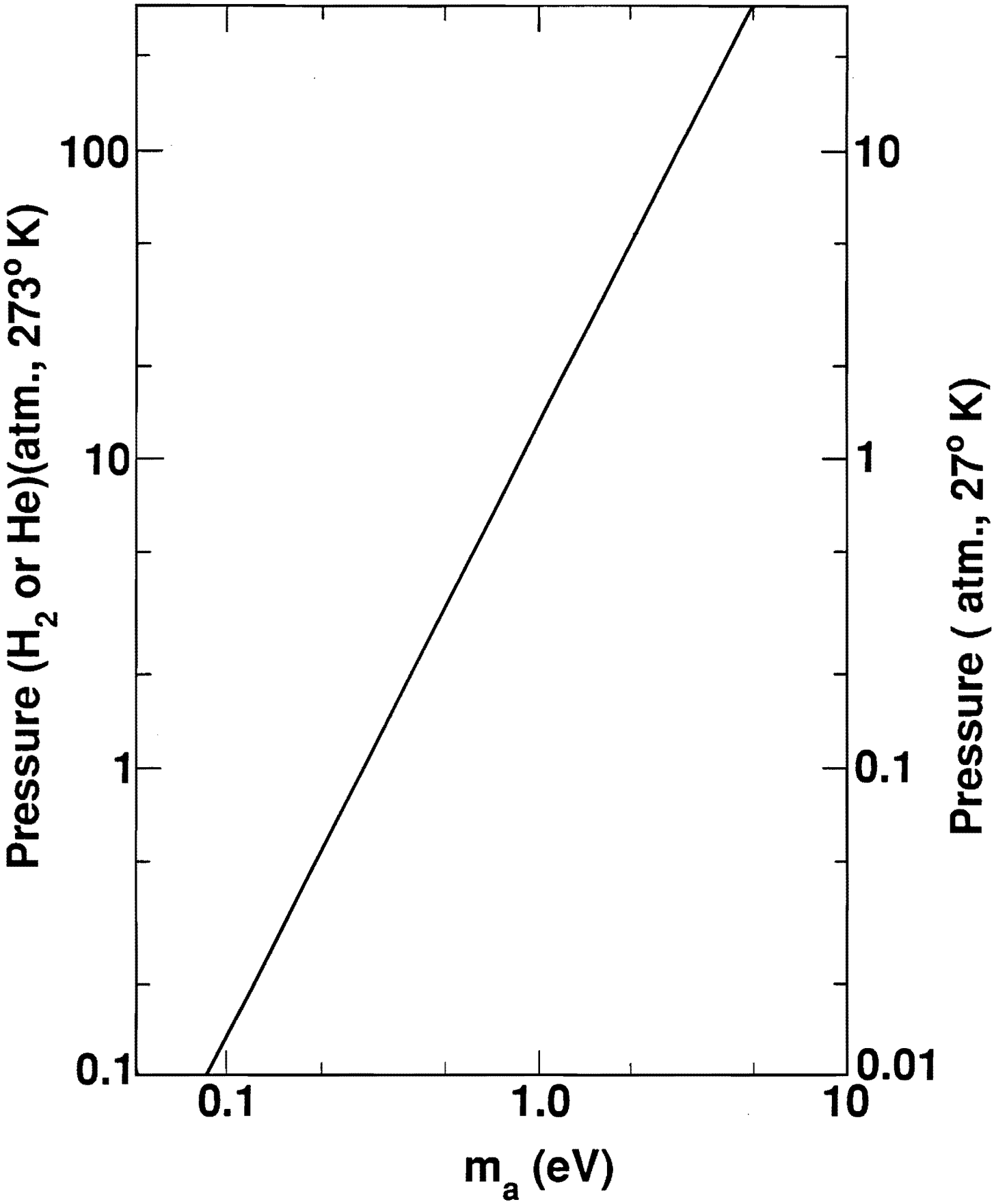
100
10
1
0.1
Pressure (H_2 or He)(atm., 273° K)
10
1
0.1
0.01
Pressure (atm., 27° K)
0.1
1.0
10
m_a (eV)

Figure 5

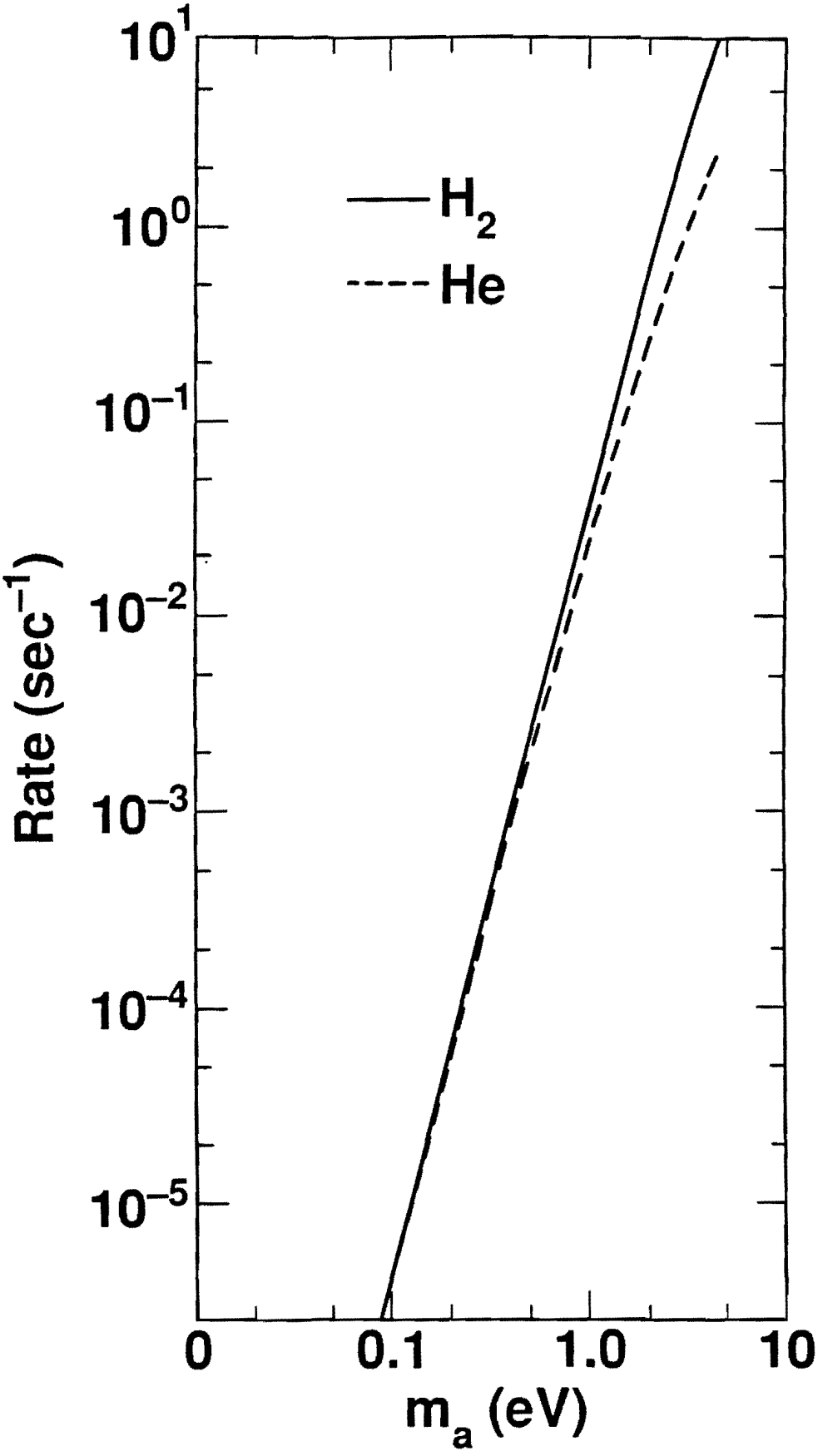

Figure 6

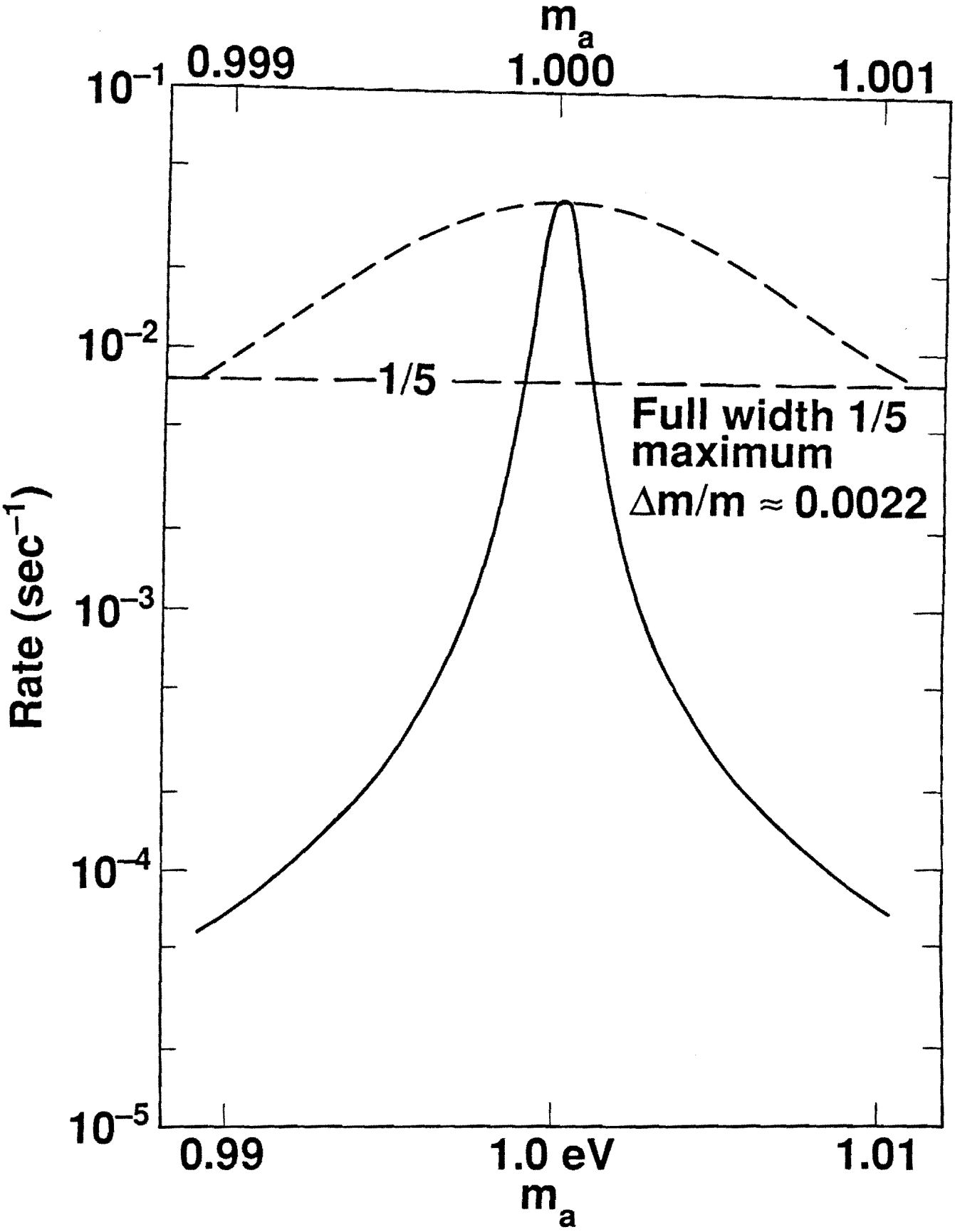
m_a
0.999
1.000
1.001
10^{-1}
10^{-2}
10^{-3}
10^{-4}
10^{-5}
1/5
Full width 1/5 maximum
$\Delta m/m \approx 0.0022$
Rate (sec^{-1})
0.99
1.0 eV
1.01
m_a

Figure 7

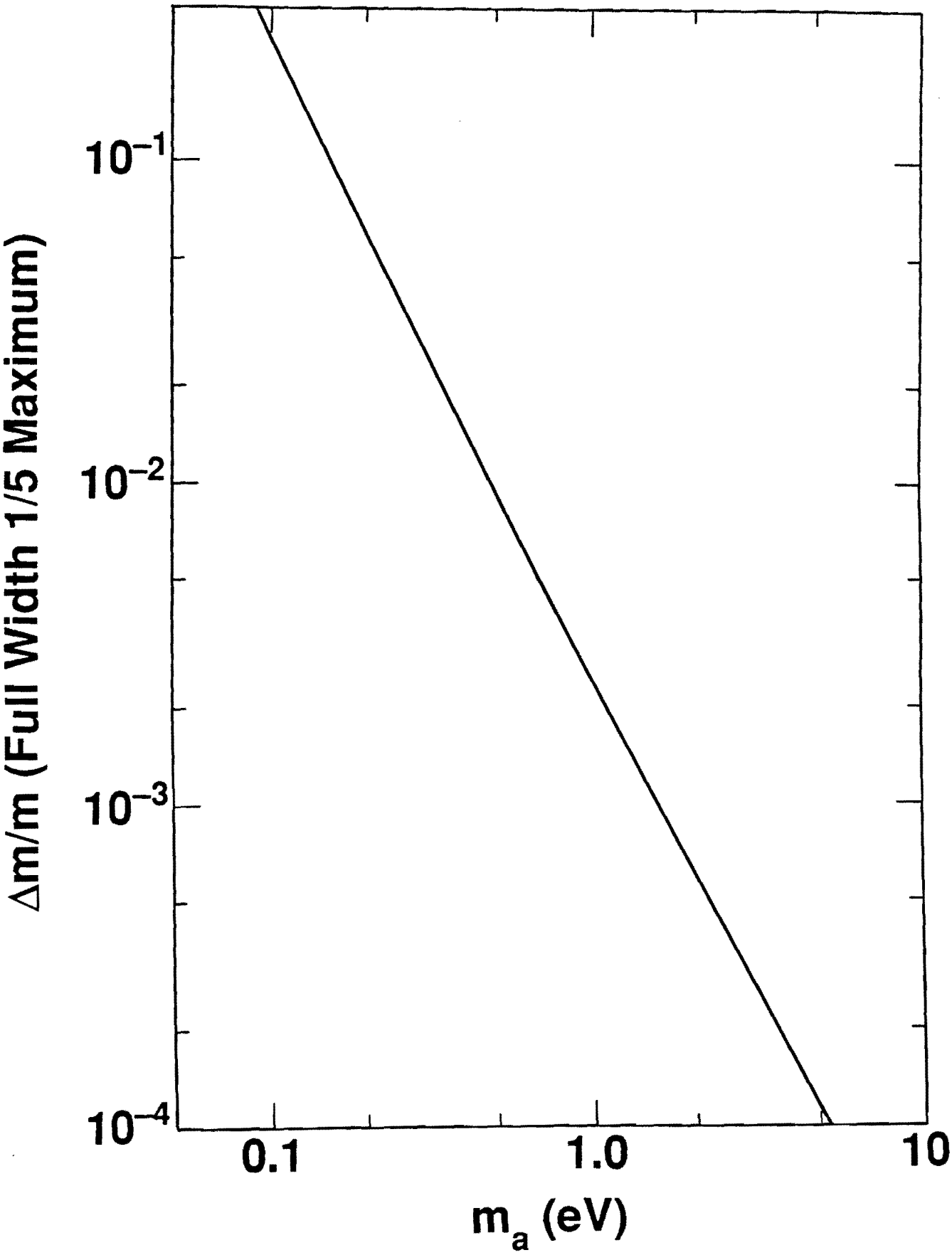

Figure 8